Adaptive Finite Element Simulations for Macroscopic and Mesoscopic Models of Steel

Alfred Schmidt, Bettina Suhr, Thilo Moshagen, Michael Wolff, Michael Böhm

Zentrum für Technomathematik, Fachbereich 3, Universität Bremen, 28334 Bremen, Germany, {schmidt, bsuhr, moshagen, mwolff, mbohm}@math.uni-bremen.de

Abstract

During heat treatment and other production processes, gradients of temperature and other observables may vary rapidly in narrow regions, while in other parts of the workpiece the behaviour of these quantities is quite smooth. Nevertheless, it is important to capture these fine structures during numerical simulations. Local mesh refinement in these regions is needed in order to resolve the behaviour in a sufficient way. On the other hand, these regions of special interest are changing during the process, making it necessary to move also the regions of refined meshes. Adaptive finite element methods present a tool to automatically give criteria for a local mesh refinement, based on the computed solution (and not only on a priori knowledge of an expected behaviour).

We present examples from heat treatment of steel, including phase transitions with transformation induced plasticity and stress dependent phase transformations. On a mesoscopic scale of grains, similar methods can be used to efficiently and accurately compute phase field models for phase transformations.

Keywords

Adaptive methods, finite element simulations, heat treatment of steel, transformation induced plasticity

1 Need for local mesh refinement - adaptive finite element methods

During production processes like heat treatment, fine structures like narrow regions (boundary or interior layers, e.g.) with high (and rapidly varying) gradients of temperature, concentration, or phase fraction fields appear, while in other parts of the workpiece the behaviour of these fields is quite smooth. It is important to capture these structures during numerical simulations, as they influence the local or global material properties during and after the process. So, a fine mesh is essential, but using a globally fine mesh can be prohibitively expensive, especially in 3D. *Local* mesh refinement in these regions is needed in order to resolve the behaviour in a sufficient way, while keeping the overall calculation feasible.

Adaptive finite element methods present a tool to automatically give criteria for a local mesh refinement, based on the computed solution (and not only on a priori knowledge of an expected behaviour). These method were introduced and studied by engineers and mathematicians starting in the late 1970s (see [Babuška, 1987], [Zienkiewicz, 1978], e.g., and [Ainsworth, 2000] for an overview). For model problems, mathematical bounds for the error between approximate and true solution can be shown, as well as quasi-optimality of the meshes generated by the adapive method. In adaptive methods, regions for local refinement are selected based on local *error indicators*, which estimate the error contribution of single mesh elements. They are computed from the discrete solution on the current mesh and known data of the problem (like material parameters and boundary values). All mesh elements where these indicators are large must be refined, while elements with very small indicators may be coarsened. The latter is important especially in time dependent simulations, when local structures may move or even vanish after some time. We show here the application of adaptive finite element methods to both macroscopic and mesoscopic models for phenomena during the heat treatment of steel.

2 Macroscopic model: Thermo-elasticity with phase changes

The linearized model of thermo-elasticity with phase transformations (for small and quasi-static deformations) including temperature T, deformation u, and phase fractions p_i is given by the following differential equations.

$$\begin{aligned} &\rho c\dot{T} - div(k\nabla T) = \rho\sum L_i \dot{p}_i \\ (1)\qquad &- div(\sigma) = 0 \\ &\dot{p}_i = f_i(p,T) \end{aligned}$$

with stress

$$(2)\qquad \sigma = \lambda\, tr(\varepsilon)I + 2\mu\varepsilon - (3\lambda + 2\mu)\{\alpha(T - T_0) + (\rho_0 - \rho)/3\rho\}I$$

and strain $\varepsilon = \frac{1}{2}(\nabla u + \nabla u^T)$. f_i is the law of phase change, and $\rho, c, k, L_i, \lambda, \mu, \alpha, T_0, \rho_0$ denote material parameters, most of them depending on temperature and/or phase. Initial and boundary conditions are defined for this system. The partial differential equations are numerically solved by a finite element method. As we want to focus in this article on aspects of the *numerical* methods, the model is kept simple here; for more elaborate models see, for example, [Wolff, 2005b]. In the remainder of this section, we show the advantages of adaptive methods in two different situations.

2.1 Boundary layers during heat treatment

We consider the temperature boundary layer during cooling of a rectangular steel workpiece in 2D. A steel model from [Wolff, 2000] was used. Being initially at a constant high temperature, the sample is cooled from outside, where one side of the rectangle is cooled stronger than the others. Figure 1 shows temperature graphs and corresponding meshes from two different times. In the beginning, the temperature is lowered mainly near the edges, leading to boundary layers. The temperature reduction near the stronger cooled side is much stronger than near the others. A good resolution of the temperature profile is required for example in order to approximate a temperature-dependent phase transformation with appearance of different constituents (pearlite, bainite, martensite, e.g.) and predict local material properties after the heat treatment. In order to numerically resolve the temperature profiles well, the mesh has to be quite fine near the boundary layers. An adaptive method based on local error indicators automatically refines the mesh where it is needed.

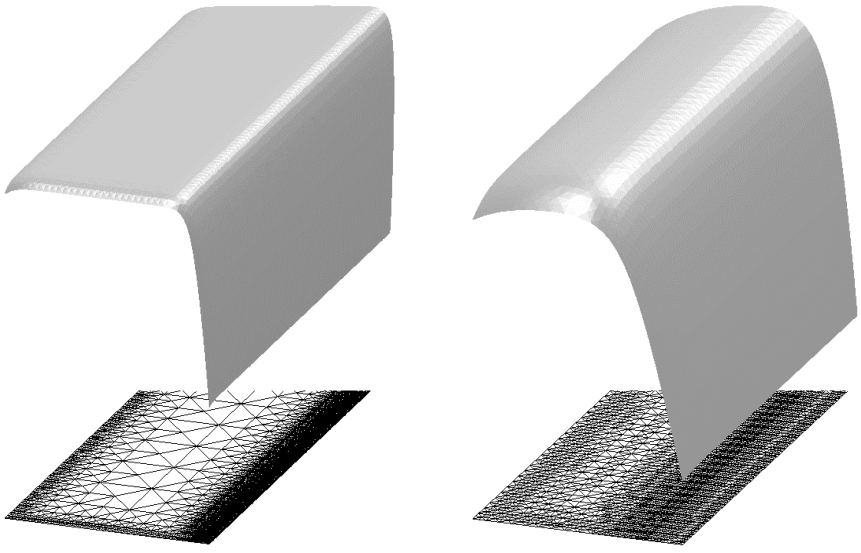

Figure 1: Quenching of a hot steel workpiece (2D): Graphs of temperature and corresponding adaptive meshes at two different times

After some time, heat diffusion leads to much smoother temperature profiles, and thus coarser meshes are sufficient to resolve the temperature near the boundary. But now a finer mesh is needed also in the interior, as temperature is no longer nearly constant there.

Naturally, similar effects occur during heat treatment of more complicated workpieces. Figure 2 shows a simple 2D and 3D geometry of a cog wheel. The simulation assumes a stronger cooling rate at the cog tips. Again, a finer mesh is essential at these places in order to approximate the temperature boundary layer and stronger deformation sufficiently well.

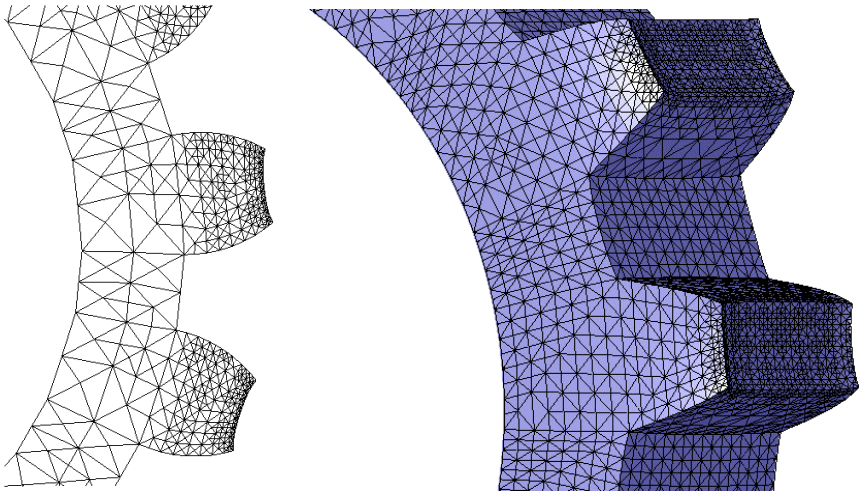

Figure 2: Heat treatment of a (simple) cogwheel in 2D and 3D, with stronger cooling of the cog tips: Adaptive meshes with emphasized deformations.

2.2 Interior layers due to phase transition in a layered material

In dilatometer experiments with heat treatment cycles for a low alloy Mn-Cr steel with banded chemical inhomogeneities, an anisotropic dilatation behaviour is observed [Hunkel, 2005]. A possible explanation is given by local effect of transformation induced plasticity (TRIP), due to internal stresses from different phase transition laws in different layers.

A common model for TRIP (compare [Mitter, 1987], [Leblond, 1989], [Fischer, 1996], e.g.) is given by splitting the total strain ε into its thermoelastic part and the one produced by TRIP, $\varepsilon = \varepsilon_{te} + \varepsilon_{TRIP}$, together with an evolution law for the latter like

$$\dot{\varepsilon}_{TRIP} = \tfrac{3}{2}\kappa\sigma^{*}\phi'(p)\dot{p}\,, \qquad \varepsilon_{TRIP}(0) = 0$$

where ϕ denotes a saturation function and σ^{*} the stress deviator. In contrast to (2) above, the stress is now $\sigma = \lambda\, tr(\varepsilon - \varepsilon_{TRIP})I + 2\mu(\varepsilon - \varepsilon_{TRIP}) - (3\lambda + 2\mu)\{\alpha(T - T_0) + (\rho_0 - \rho)/3\rho\}I$ and depends only on the thermoelastic strain. κ is a material parameter which can be determined by simple experiments [Wolff, 2005a]; see [Dalgic, 2003], [Dalgic, 2004] for data. Again, the model is kept simple here, see [Wolff, 2004], [Wolff, 2005d] for more complex models, including back stress e.g., discussion and literature. The numerical method used here was described in [Schmidt, 2003b].

As a model problem, we consider here a small cuboid (length:width:height $= \sqrt{2}:1:1$) piece of material with 3 or 5 equally wide layers of alternating phase transition properties, for an austenite-pearlite transition during cooling. The phase transition in the even layers occurs at a higher temperature, and thus earlier during cooling, than in the other layers. Due to different densities of the constituents, high stresses appear near the inner band boundaries during the phase transitions. This leads to strong TRIP effects. The cooling conditions are uniform over the whole boundary, so there are no asymmetries due to the boundary conditions.

Figure 3 shows adaptive meshes and deformations (emphasized by factor 100) from a cooling simulation (from 750°C to 600°C in 50 seconds, approximately). The final triangulation has approximately 300'000 tetrahedra. In Figure 4, the final (emphasized) deformed 3D geometry is shown.

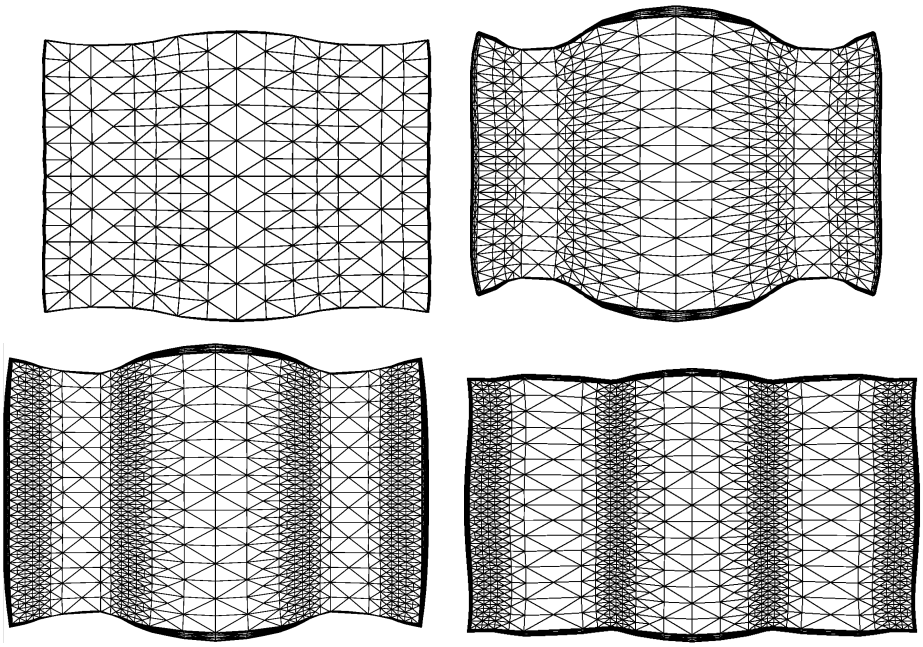

Figure 3: Simulated heat treatment of layered material: Adaptive meshes and deformation (scaled by factor 100) at times t=25s, 30s (top) and t=35s, 40s (bottom).

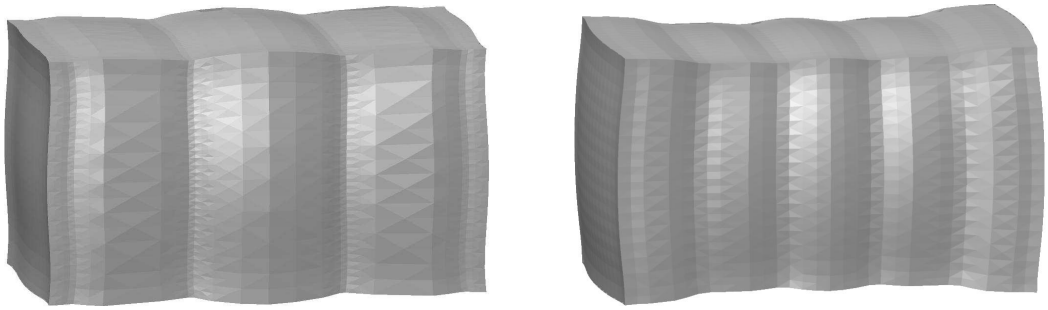

Figure 4: Simulated heat treatment of layered material: Final 3D geometry (3 and 5 layers).

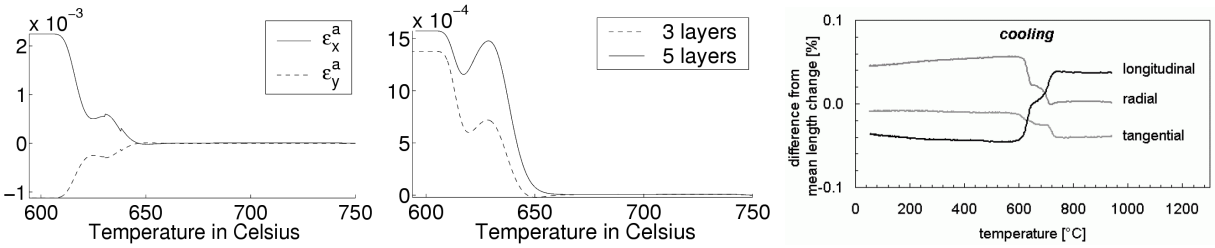

Figure 5: Simulated heat treatment of layered material. Left: Relative length changes in longitudinal and transversal directions (for 3 layers). Middle: Comparison of 3 and 5 layers. Right: Experimental data.

The anisotropic length changes during the simulation are presented in Figure 5. The values shown here express the TRIP effect and are computed by

$$\varepsilon_x^a = \varepsilon_x - (\varepsilon_x + \varepsilon_y + \varepsilon_z)/3, \qquad \varepsilon_y^a = \varepsilon_y - (\varepsilon_x + \varepsilon_y + \varepsilon_z)/3,$$

where $\varepsilon_x, \varepsilon_y, \varepsilon_z$ are the relative length changes in x, y, z directions, evaluated at a vertex of the geometry. Due to symmetry, $\varepsilon_y = \varepsilon_z$. These curves are nearly independent on the actual size of the cuboid, we ran simulations for lengths 8mm, 0.8mm, and 0.08mm; the different curves would not be distinguishable from each other. For more layers, the anisotropic TRIP effect gets stronger, see the middle of Figure 5, which shows ε_x curves for 3 and 5 layers.

At least qualitatively, these results are quite similar to the experiments in [Hunkel, 2005], see right hand of Figure 5 (due to the layered geometry, our y, z directions correspond to the longitudinal one in the experiment). Thus, TRIP effects are a possible explanation for these anisotropic deformations. For quantitative studies, further investigations with material parameters corresponding to the steel considered there will be done in the future.

3 Mesoscopic modelling of transformation phenomena

As empiric macroscopic models for phase transition and related effects are still not satisfactory, the derivation of new macroscopic (or multi-scale) models from mesoscopic considerations, models, and simulations may lead to better agreement with experiments. In the macroscopic models considered above, mixtures of different constituents are possible and their relative amount is given by phase fraction functions $p_i(x,t)$. Looking at the mesoscopic scale of single or multiple grains, one observes pure phases in (parts of) grains with (relatively) sharp phase boundaries.

For such phase transitions, sharp-interface or diffuse-interface models are appropriate. While sharp-interface models are problematic when the interface changes topology, like in case of phase nucleations, diffuse-interface models can easily handle such topology changes. Phase field models are based on the assumption of a smooth phase variable, which varies rapidly between nearly constant values, representing pure phases, in a narrow transition region of width $O(\delta)$. This transition region represents a diffuse interface, which is moving during phase transition.

Here we aim at phase field models for solid-solid phase transitions in steel, including the influence of stress on the phase transformation. In the phase field model, the ordinary differential equation $\dot{p} = f(T, p)$ in (1) is replaced by a partial differential equation

$$\delta(\dot{p} - a\Delta p) + \frac{1}{\delta}\Psi'(p) = f \ ,$$

where δ is a small parameter and Ψ is a potential with two minima at 0 and 1, the values for the pure phases. We use a double obstacle potential [Blowey, 1993]. Depending on the model, the right hand side f may depend on concentration, temperature, and stress or strain. For this example, we consider a simple temperature-driven phase transition with a modification which allows for a stress-dependent transformation (compare [Paret, 2001], e.g., for a purely stress-dependent model).

$$f = \gamma T - c \cdot \sigma : \sigma \ .$$

For $c > 0$, the negative sign in front of the stress term leads to an accelerated phase transition. Numerical (very preliminary) results show that it is possibile to include stress dependent effects into the mesoscopic transformations by such a simple modification of the underlying energy functional. For some (macroscopic) ideas of more elaborate stress dependencies, see [Wolff, 2005c]. We want to simulate the temperature- and stress-driven phase transition in a single 2D six-sided grain. Cooling from the left side results in the nucleation of the new phase in the left corner. Temperature gradients and density changes leads to interior stresses, which accelerate the phase transition when $c > 0$. For phase variable and stress, we assume for this simple test case here the natural (homogeneous) boundary conditions on the grain boundary.

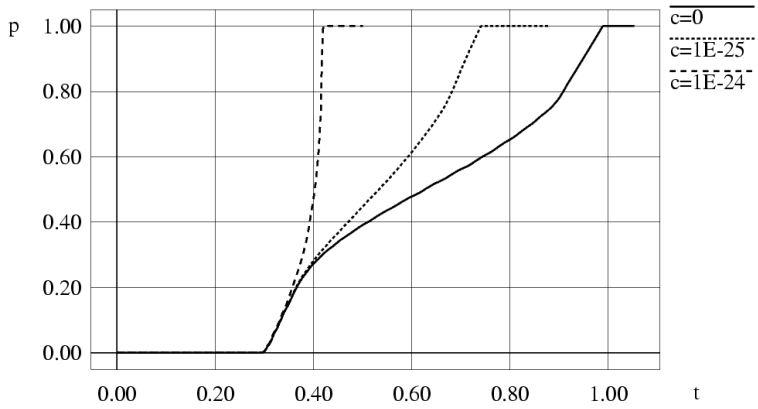

Figure 6: Comparison of volume fractions over time for different influence of stress (different c).

We use a finite element discretization and an adaptive method based on error indicators from [Chen, 2005], [Schmidt, 2003a]. In Figure 6, we show the evolution of the relative volume of the growing phase inside the grain. Three curves show the phase transitions for $c = 10^{-24}$, $c = 10^{-25}$, and $c = 0$. The figure shows that, depending on the parameters, such models can lead to very strongly accelerated phase transitions.

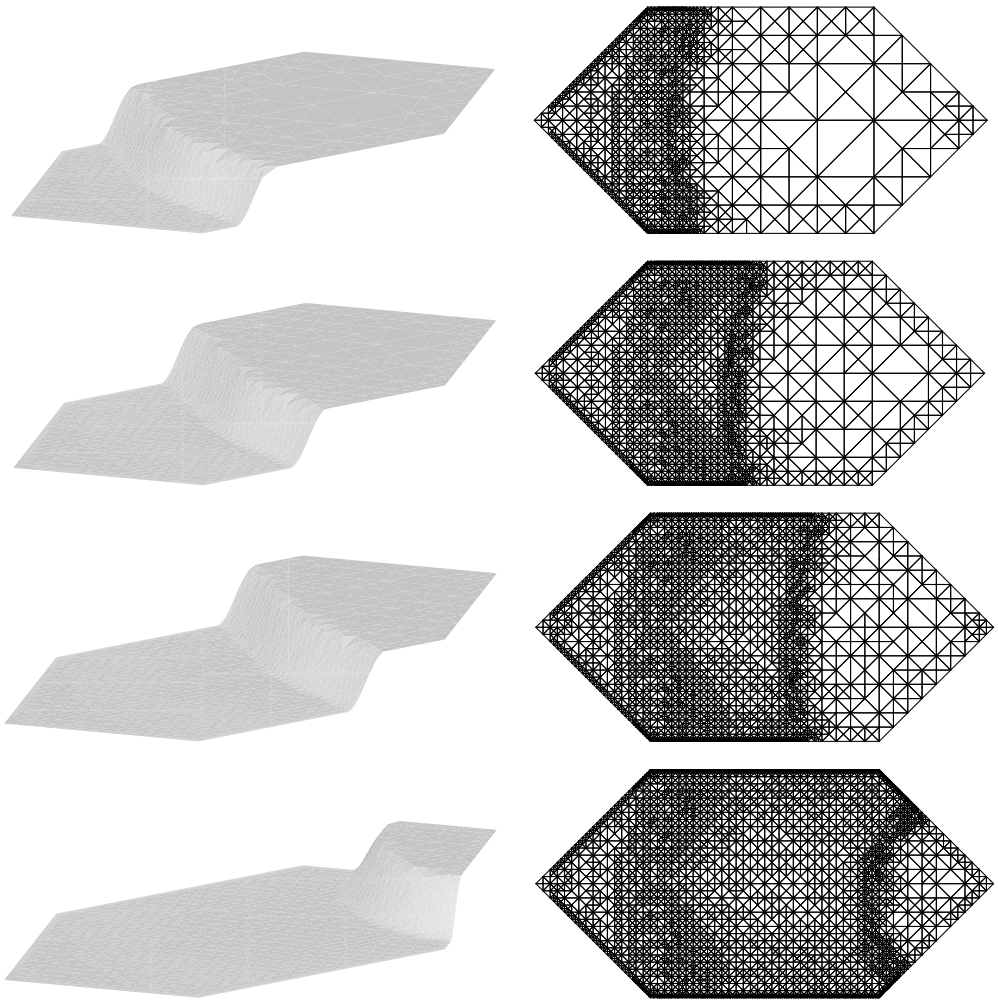

Figure 7: Graphs of phase variable and corresponding meshes at time t=0.4, 0.5, 0.6, 0.7.

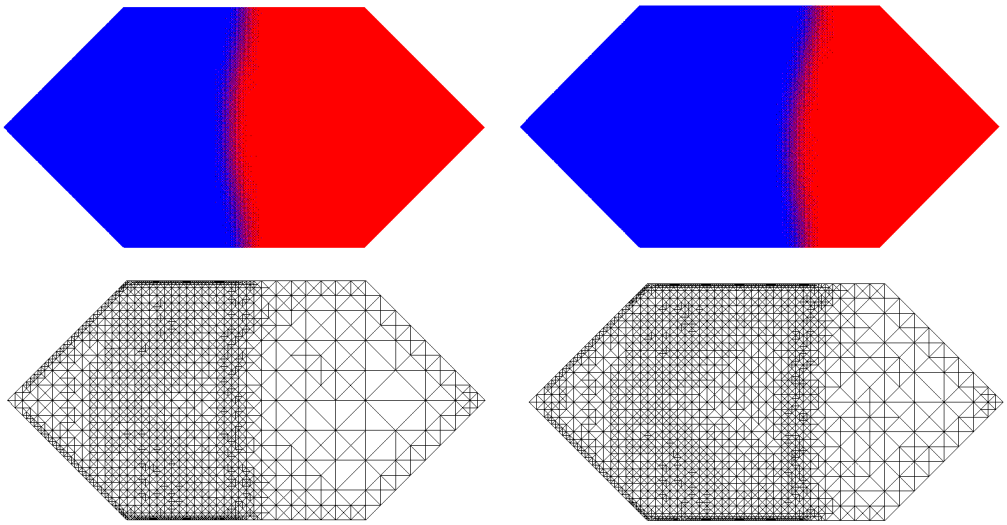

Figure 8: Comparison of simulations without ($c = 0$, left) and with stress ($c = 10^{-25}$, right): Phases at time t=0.6 and corresponding meshes.

Figure 7 shows values of the phase variable (corresponding to the untransformed phase) and corresponding finite element meshes from a simulation with influence of stress ($c = 10^{-25}$). In Figure 8, we compare phase distributions at the same time from simulations without ($c = 0$) and with ($c = 10^{-25}$) strain. Under influence of strain, the phase boundary has moved farther.

The adaptive method automatically refines the mesh in the moving transition region, where the phase variable is not constant, so that it can be approximated well. This highly refined region is coarsened again, when the transition region has moved forward. Additional refinement is due to variations in the temperature and deformation fields. These simulations are still part of a work in progress. Multi-grain configurations and more elaborate and realistic parameters and boundary conditions will be considered in the future.

4 Conclusion

We have shown some examples, where local phenomena like boundary layers, interior layers, and phase transition regions appear naturally in models and simulations for the heat treatment of steel. The adaptive finite element method presents an automatic tool for numerical simulations, and produces locally refined meshes where needed for accurate computations. Especially in 3D, computations of similar accuracy would be too costly when not using local refinements, but a globally refined mesh.

Acknowledgement

This work has partially been supported by the Deutsche Forschungsgemeinschaft (DFG) via the Collaborative Research Centre SFB 570 “Distortion Engineering” at the University of Bremen.

All numerical simulations presented in this article were performed using the adaptive finite element toolbox ALBERTA [Schmidt, 2005]. The 2D and 3D figures were produced with the package Grape [Grape, 1995].

We thank one of the referees for valuable comments and hints.

References

Ainsworth, M.; Oden, J. T.: A Posteriori Error Estmation in Finite Element Analysis. Wiley, 2000.

Babuška, I.; Rheinboldt, W. C.: A posteriori error estimates for the finite element method. Internat. J. Numer. Methods Engrg. 12, 1597-1615, 1987.

Blowey, J.; Elliott, C.: Curvature dependent phase boundary motion and parabolic double obstacle problems. In Ni, Wei-Ming et al. (Eds.): Degenerate diffusions. IMA Vol. Math. Appl. 47, 19-60, 1993.

Chen, Z.; Nochetto, R. H.; Schmidt, A.: Adaptive finite element methods for diffuse interface models. In preparation, 2005.

Dalgic, M.; Löwisch, G.: Werkstoffkennwerte für die Simulation von Wärmebehandlungsvorgängen, In: Buchholz, O.W.: Geisler, S. (Eds): Proceedings of the conference Werkstoffprüfung 2003, Bad Neuenahr-Ahrweiler, Germany, Dec 4-5, 2003, Verlag Stahleisen, Düsseldorf, 2003.

Dalgic, M.; Löwisch, G.: Einfluss einer aufgeprägten Spannung auf die isotherme, perlitische und bainitische Umwandlung des Wälzlagerstahls 100Cr6. HTM 59(1), p. 28-34, 2004.

Fischer, F. D.; Sun, Q.P.; Tanaka, K.: Transformation-induced plasticity (TRIP). Appl. Mech. Rev. 49, 317-364, 1996.

Grape: Graphics programming environment. Manual, Version 5, SFB256 Univ. Bonn, 1995.

Hunkel, M.; Frerichs, F.; Prinz, C.; Surm, H.; Hoffmann, F.; Zoch, H.-W.: Size change due to anisotropic dilatation behavior of a low alloy Mn-Cr steel. In preparation, 2005.

Leblond, J. B., Devaux, J., Devaux, J. C.: Mathematical modelling of transformation plasticity in steels. I: Case of ideal-plastic Phases. Int. J. Plasticity 5, 551-572, 1989.

Mitter, W.: Umwandlungsplastizität und ihre Berücksichtigung bei der Berechnung von Eigenspannungen. Materialkundlich-technische Reihe 7, Gebr. Borntraeger, Berlin, Stuttgart, 1987.

Paret, J.: Phase-field model of stressed incoherent solid-solid interfaces. Eprint arXiv:cond-mat/0110378, 2001.

Schmidt, A.: A multi-mesh finite element method for phase field simulations. In Emmerich, H.; Nestler, B.; Schreckenberg, M. (Eds.): Interface and Transport Dynamics - Computational Modelling. Springer LNCSE 32, pp. 208-217, 2003a.

Schmidt, A.; Wolff, M.; Böhm, M.: Numerische Untersuchungen für ein Modell des Materialverhaltens mit Umwandlungsplastizität und Phasenumwandlungen beim Stahl 100Cr6. Univ. Bremen, Berichte aus der Technomathematik, Report 03-13, 2003b.

Schmidt, A.; Siebert, K. G.: Design of adaptive finite element software: The finite element toolbox ALBERTA. Springer LNCSE Series 42, 2005.

Wolff, M.; Bänsch, E.; Böhm, M.; Davis, D.: Modellierung der Abkühlung von Stahlbrammen. Univ. Bremen, Berichte aus der Technomathematik, Report 00-07, 2000.

Wolff, M.; Böhm, M.; Dalgic, M.; Löwisch, G.; Lysenko, N.; Rath, J.: Parameter identification for a TRIP model with back stress. To appear in Computational Materials Sciences, proceedings of the conference IWCMM14, Goa, India, 2004.

Wolff, M.; Böhm, M.; Löwisch, G.; Schmidt, A.: Modelling and testing of transformation-induced plasticity and stress-dependent phase transformations in steel via simple experiments. Computational Materials Sciences 32, 604-610, 2005a.

Wolff, M.; Böhm, M.; Schmidt, A.: A thermodynamically consistent model of the material behaviour of steel including phase transformations, classical and transformation-induced plasticity. In: Wang, Y.; Hutter, K.: Trends in Applications of Mathematics to Mechanics, Shaker Verlag, Aachen, pp. 591-601, 2005b.

Wolff, M.; Böhm, M.; Schmidt, A.: Modelling of steel phenomena and its interactions - an internal-variable approach, submitted to proceedings of the 1st International Conference on Distortion Engineering, Bremen, Germany, 14-16 September, 2005c.

Wolff, M.; Böhm, M.; Dalgic, M.; Löwisch, G.; Rath, J.: TRIP and phase evolution for the pearlitic transformation of the steel 100Cr6 under step-wise loads. Submitted to proceedings of the 1st International Conference on Distortion Engineering, Bremen, Germany, 14-16 September, 2005d.

Zienkiewicz, O. C.; Zhu, J. Z.: A simple error estimator and adaptive procedure for practical engineering analysis. Internat. J. Numer. Methods Engrg. 24, 337-357, 1987.